Available online at www.sciencedirect.com
SCIENCE DIRECT®
Journal of Magnetic Resonance 176 (2005) 107–114
JMR Journal of Magnetic Resonance
www.elsevier.com/locate/jmr

Communication

A continuous phase-modulated approach to spatial encoding in ultrafast 2D NMR spectroscopy

Assaf Tal, Boaz Shapira, Lucio Frydman *

Department of Chemical Physics, Weizmann Institute of Science, 76100 Rehovot, Israel

Received 28 February 2005; revised 2 May 2005
Available online 9 June 2005

Abstract

Ultrafast 2D NMR replaces the time-domain parametrization usually employed to monitor the indirect-domain spin evolution, with an equivalent encoding along a spatial geometry. When coupled to a gradient-assisted decoding during the acquisition, this enables the collection of complete 2D spectra within a single transient. We have presented elsewhere two strategies for carrying out the spatial encoding underlying ultrafast NMR: a discrete excitation protocol capable of imparting a phase-modulated encoding of the interactions, and a continuous protocol yielding amplitude-modulated signals. The former is general but has associated with it a number of practical complications; the latter is easier to implement but unsuitable for certain 2D NMR acquisitions. The present communication discusses a new protocol that incorporates attractive attributes from both alternatives, imparting a continuous spatial encoding of the interactions yet yielding a phase modulation of the signal. This in turn enables a number of basic experiments that have shown particularly useful in the context of in vivo 2D NMR, including 2D *J*-resolved and 2D H,H-COSY spectroscopies. It also provides a route to achieving sensitivity-enhanced acquisitions for other homonuclear correlation experiments, such as ultrafast 2D TOCSY. The main features underlying this new spatial encoding protocol are derived, and its potential demonstrated with a series of phase-modulated homonuclear single-scan 2D NMR examples.

Keywords: Ultrafast 2D NMR; Continuous spatial encoding; Chirped RF irradiation; Sensitivity enhancement; In vivo 2D MRS

1. Introduction

Two-dimensional (2D) spectroscopy fulfills a central role in the application of nuclear magnetic resonance (NMR) to Chemistry, Biochemistry, and Medicine [1–3]. 2D NMR experiments separate and correlate spin interactions along independent frequency domains, providing an enhancement in resolution and an information that is unavailable in unidimensional spectral counterparts. Bidimensional correlations are traditionally imposed by monitoring signals as a function of two variables: an evolution time t_1 encoding the indirect-domain Ω_1 interactions, and an acquisition time t_2 measuring the direct-domain frequencies Ω_2. As in this protocol t_1 constitutes a time parameter that gets incremented in a scan-by-scan fashion, numerous individual transients will have to be collected for completing a 2D NMR acquisition regardless of sensitivity considerations. Recently, however, an "ultrafast" approach has been proposed that departs from this scheme, and enables the acquisition of 2D NMR spectra within a single transient [4–6]. At the heart of this single-scan approach lies replacing the t_1 encoding, which will necessarily demand the performance of several experiments for an appropriate digitization, with an analogous spatial encoding of the interactions. Given present-day NMR hardware this spatial encoding is most conveniently imparted via the application of a suitable G_e magnetic field gradient

* Corresponding author. Fax: +972 8 9344123
E-mail address: lucio.frydman@weizmann.ac.il (L. Frydman).

1090-7807/$ - see front matter © 2005 Elsevier Inc. All rights reserved.
doi:10.1016/j.jmr.2005.05.009

along the $\hat{z}$ direction, in combination with a series of selective radiofrequency (RF) pulses. For instance, the scheme illustrated in Fig. 1A, combining a train of N_1 bipolar gradients and RF pulses spread out between $+\gamma_e G_e L/2$ and $-\gamma_e G_e L/2$ offsets, will succeed in endowing spins spread over a length L with a spatially dependent evolution phase

$$\{\phi_e(z_j) = C\Omega_1(z_j + L/2)\}_{1\leqslant j\leqslant N1}, \tag{1}$$

where $C = \Delta t_1 \gamma_e G_e/\Delta O \approx t_1^{\max}/L$ is a spatio-temporal ratio under the experimentalist's control. This equation represents a winding of the site's magnetization which, following a conventional mixing pulse sequence, will be coherently transferred into an observable species. The ultrafast 2D NMR protocol then reads this winding out via the action of an acquisition field gradient G_a, leading to

$$S(k,t_2) = \int_{\Omega_2}\left\{\int_{\Omega_1} I(\Omega_1,\Omega_2)\left[\sum_{j=1}^{N_1} A(z_j)\,\mathrm{e}^{\mathrm{i}C\Omega_1(z_j+L/2)}\,\mathrm{e}^{\mathrm{i}kz_j}\right]\mathrm{d}\Omega_1\right\} \times \mathrm{e}^{\mathrm{i}\Omega_2 t_2}\,\mathrm{d}\Omega_2. \tag{2}$$

In this equation $k = \gamma_a \int_0^t G_a(t')\,\mathrm{d}t'$ is an acquisition wavenumber, $A(z_j)$ is a weighting function depending on the z density profile of the spins as well as on details of the spin excitation [7,8], and $I(\Omega_1,\Omega_2)$ is the 2D distribution one is attempting to extract. As can be appreciated from the bracketed sum within Eq. (2) the acquisition wavenumber performs an analog Fourier transform (FT) of the evolution encoded along the spatial domain, leading to Ω_1-specific echoes whenever $k = -C\Omega_1$. The position of such echoes will thus reveal the internal evolution frequencies, making the k wavenumber equivalent to an indirect-domain v_1 frequency axis. Furthermore, this gradient-driven readout can be undone and reapplied numerous times during the course of an acquisition simply by oscillating the sign of the G_a gradient, allowing one to monitor the direct-domain Ω_2 frequencies via the phase modulations that they will impart on the multiple k-domain echoes then resulting as a function of t_2. Either a conventional or an interlaced FT along the direct domain [4,9] will thus lead to a 2D NMR spectrum within a single scan.

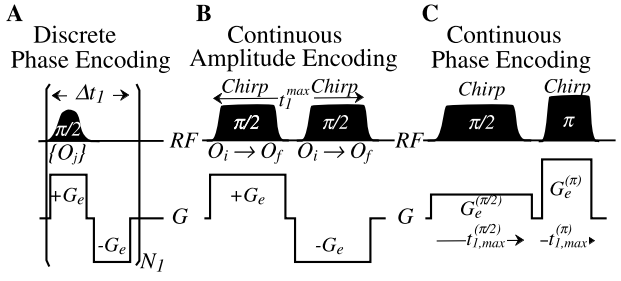

Fig. 1. Schemes capable of affording the spatial encoding pattern required for ultrafast 2D NMR acquisitions. (A) Discrete phase-modulated encoding protocol composed of a train of N_1RF pulses, applied at constant frequency increments $\Delta O = (\gamma_e G_e L)/(N_1 - 1)$ in combination with multiple $\pm G_e$ gradient oscillations. (B) Continuous amplitude-modulated scheme where a pair of identical frequency-swept irradiation pulses is applied over a range $\approx\gamma_e G_e L$ in combination with a single bipolar gradient, to achieve the storage of a $\cos(C\Omega_1 z)$ longitudinal magnetization pattern. (C) New encoding scheme proposed in the present study, capable of yielding a phase-modulated $\exp(\mathrm{i}C\Omega_1 z)$ transverse evolution without requiring the application of rapidly oscillating $\pm G_e$ gradients. Schemes are illustrated for a single-channel excitation for the sake of simplicity; see the text for further definitions.

Though general in terms of its overall principles and capabilities, the discrete encoding mode just described poses a number of practical complications. One concerns its need for applying N_1 switching field gradients to be carefully timed with the RF irradiation. While this procedure may not be challenging to implement in state-of-the-art spectroscopy systems where the rise and fall times of oscillating gradients are nearly negligible, quite different has been our experience when operating in wider-bore imaging-oriented hardware. Particularly deleterious in these instances become the relatively slow gradient switching times and the onset of parasitic eddy current effects, which conspire against all the delicate timings and balances underlying the spatial encoding process, and often result in broad k-domain echoes. Further complications arise from the nature of the encoding itself, which being discrete will subject the indirect-domain k/v_1 peaks to "ghosting" effects related to a fold-over of the echoes, as well as to intra-slice dephasing ("enveloping") effects [5,8]. In order to deal with these various complications we have recently proposed a continuous approach to the spatial encoding that, unlike its discrete counterpart, is of straightforward implementation in both spectroscopic and in vivo-type MRI settings [10]. This protocol involves the application of an initial frequency-swept $\pi/2$ pulse that executes a sequential excitation of spins throughout the sample while in the presence of a $+G_e$ gradient, followed by an identical chirped pulse acting in the presence of a $-G_e$ gradient whose goal is to carry out a time-reversed storage of the evolved spin coherences (Fig. 1B). Since the gradient inversion makes the last spins to be excited the first ones to be stored the quadratic spatial evolution otherwise imparted by the G_e gradient cancels out, giving the amplitude of the stored magnetization a spatial encoding of the type

$$M_z(z) = A(z)\cos[C\Omega_1(z + L/2) + \theta]. \tag{3}$$

Although the Ω_1-encoding thus imparted is—as required by the ultrafast principle—linear in space, this amplitude modulation is incompatible with certain 2D experiments exploited in clinical NMR spectroscopy (MRS) settings, including the 2D J-resolved sequence [11–13] and the standard two-pulse H,H-COSY sequence [1–3,14,15]. The chemical shift/J-coupling correlations resulting from the first of these experiments

requires a simple in-plane π-pulse reversal of the transverse spin magnetization, and its value derives from the fact that in combination with a data shearing it can in essence achieve an effective homonuclear spin decoupling along one of the spectral dimensions. This yields a resolution improvement that, though not appreciable by the standards of modern high-field biomolecular NMR, is valuable in the low fields usually employed in whole-body MRS. The second of the experiments mentioned will correlate, as in the case of TOCSY [16], chemical shifts of neighboring protons via their mutual *J*-couplings. And while it is less informative and its peaks are more poorly shaped than those of TOCSY, H,H-COSY is advantageous in that its connectivities are imparted by a single π/2 pulse rather than via long-trains of π rotations. This in turn has made the single-quantum transfer in COSY a preferred route to create homonuclear correlations in MRI systems characterized by low B_1 homogeneities. Evidently, the excite/store RF combination underlying the amplitude modulation in Eq. (3) will not succeed in yielding the single-quantum coherence transformations demanded by either one of these two experiments. Moreover, the excite/store amplitude-modulated approach in Fig. 1B will also leave beyond its realm ultrafast acquisitions relying on sensitivity-enhanced schemes [17–19], a widely used 2D NMR strategy whereby signal-to-noise enhancements are achieved owing to a combined manipulations of *two* orthogonal spin coherence components. In response to these various limitations, the goal of the present communication is to introduce a continuous spatial encoding variant capable of affording the in-plane phase-sensitive manipulations required by various single-scan 2D NMR schemes, while at the same time avoiding the need for reverting to a train of switching $\pm G_e$ gradients.

2. A continuous, phase-modulated spatial encoding scheme

The new variant hereby proposed replaces the second, storage portion of the spatial encoding in Fig. 1B, by a chirped pulse that acts as a spatially dependent π rotation of the spins—leaving at its conclusion magnetizations that are still within the transverse *x*–*y* planes of their corresponding Bloch spheres (Fig. 1C). To appreciate how the resulting π/2−π pulse combination operates we proceed along the lines elaborated in [10], yet making a provision for the possibility of manipulating spins using different gradients $G_e^{(\pi/2)}, G_e^{(\pi)}$ over unequal times $t_1^{(\pi/2)}, t_1^{(\pi)}$ during the course of their encoding. Further, we shall consider for simplicity at this point that the spin ensemble is subject solely to an internal Ω_1 chemical shift interaction, and that for either $P = \pi/2$ or π nutation pulses the RF is swept between initial and final frequency offsets $|O_i^{(P)} - O_f^{(P)}| = |\gamma_e G_e^{(P)} L|$ at a constant rate $|R^{(P)}| = |\gamma_e G_e^{(P)} L / t_{1,\max}^{(P)}|$—and thus making the region involved in the manipulations L for both π/2 and π sweeps.

As the offset of the initial π/2 excitation pulse is varied and longitudinal magnetizations become transverse, spins at a particular position z will begin accruing phases as a result of (i) their chemical shift precession, (ii) the action of the $G_e^{(\pi/2)}$ gradient, and (iii) the unavoidable phase incrementation resulting as a consequence of the frequency chirping [10,20]. Apart from an arbitrary hardware-defined phase factor, the spatial dependence of the magnetization resulting at the conclusion of the first π/2 chirp will then be given by a phase possessing constant, linear, and quadratic terms, according to

$$\Phi^{(\pi/2)}(z) = \frac{t_{1,\max}^{(\pi/2)}}{2}\left(\Omega_1 + \frac{\gamma_e G_e^{(\pi/2)} L}{4}\right) + \frac{t_{1,\max}^{(\pi/2)}}{L} \times \left[\left(\frac{\gamma_e G_e^{(\pi/2)} L}{2}\right) - \Omega_1\right] z - \frac{\gamma_e G_e^{(\pi/2)} t_{1,\max}^{(\pi/2)}}{2L} z^2 \tag{4}$$

whereas the constant term in this expression will only affect the phasing of the resulting indirect-domain peaks and the linear term is as desired, the quadratic evolution will prevent the formation of homogeneous echo peaks during the course of the signal acquisition. It is thus necessary to somehow get rid of this contribution. A variety of approaches are available for doing so, including, the use of a second storage π/2 chirped pulse (Fig. 1B), or the application of a free evolution period under the action of a quadratic z^2-type gradient (something which would in turn require specialized hardware). The alternative introduced in Fig. 1C is different from either one of these options and it involves flipping the phases of the spin coherences via the application of a chirped π pulse, whose amplitude is set to suit either the sudden or adiabatic regimes [21]. To visualize how this second RF sweep can achieve the cancelation of the quadratic z^2-term in Eq. (4) we shall assume, as for the π/2 analysis, that this π pulse only addresses spins when its time-dependent offset $O[\tau^{(\pi)}]$ matches the species' spatially dependent resonance frequencies $\gamma_e G_e^{(\pi)} z + \Omega_1$. At which time its effects will be to bring an immediate inversion of the relative phase subtended between the excited spin packet and the axis along which the RF is applied, as would be the case for an ideal π pulse of negligible duration. Following this sudden π flip the spin evolution will be assumed to proceed unaltered under the action of the internal and gradient-derived shifts for another period $t_{1,\max}^{(\pi)} - \tau^{(\pi)}$, until the completion of the π sweep. Given that the instant at which this second RF sweep will address a particular z position is given by

$$\tau^{(\pi)}(z) = \frac{-O_i^{(\pi)} - \gamma_e G_e^{(\pi)} z + \Omega_1}{R^{(\pi)}} \tag{5}$$

it follows that apart from a constant phase factor, the overall evolution undergone until the completion of all RF irradiation will be

$$\begin{aligned}\Phi(z) &= \Phi^{(\pi)}(z) - \Phi^{(\pi/2)}(z)\\ &= [t_{1,\max}^{(\pi)} - \tau^{(\pi)}(z)](\gamma_e G_e^{(\pi)} z + \Omega_1)\\ &\quad + 2\int_o^{\tau^{(\pi)}(z)} O(t')\,\mathrm{d}t' - \tau^{(\pi)}(z)\cdot(\gamma_e G_e^{(\pi)} z + \Omega_1)\\ &\quad - \Phi^{(\pi/2)}(z). \end{aligned} \tag{6a}$$

Simple algebra reveals that this overall evolution phase will once again contain constant, linear, and quadratic spatial contributions, according to

$$\begin{aligned}\Phi(z) = &\left[-\frac{t_{1,\max}^{(\pi)}}{4}\gamma_e G_e^{(\pi)} L - \frac{t_{1,\max}^{(\pi/2)}}{2}\left(\Omega_1 + \frac{\gamma_e G_e^{(\pi/2)} L}{4}\right)\right]\\ &+ \left[\frac{\gamma_e}{2}(4t_{1,\max}^{(\pi)} G_e^{(\pi)} - t_{1,\max}^{(\pi/2)} G_e^{(\pi/2)}) + (t_{1,\max}^{(\pi/2)} - 2t_{1,\max}^{(\pi)})\frac{\Omega_1}{L}\right]\\ &\cdot z + \left[\frac{t_{1,\max}^{(\pi/2)} G_e^{(\pi/2)} - 2t_{1,\max}^{(\pi)} G_e^{(\pi)}}{2L}\right]\cdot z^2. \end{aligned} \tag{6b}$$

The gist of the refocusing process comes with the realization that the two variables involved in the π chirp, $t_{1,\max}^{(\pi)}$ and $G_e^{(\pi)}$, provide sufficient freedom for removing the quadratic contribution that arises from the initial π/2 pulse, while preserving a linear spatial encoding carrying the form $C\Omega_1 z$ carrying the internal coupling information. Essential for achieving this refocusing is setting

$$t_{1,\max}^{(\pi/2)} G_e^{(\pi/2)} = 2t_{1,\max}^{(\pi)} G_e^{(\pi)}; \tag{7}$$

under this precondition the overall phase evolution in Eqs. (6a) and (6b) can be rewritten as

$$\begin{aligned}\Phi(z) = &-\frac{t_{1,\max}^{(\pi/2)}}{2}\left(\Omega_1 + \frac{\gamma_e G_e^{(\pi/2)} L}{2}\right)\\ &+ \gamma_e\left[\frac{t_{1,\max}^{(\pi/2)} G_e^{(\pi/2)}}{2} + \frac{t_{1,\max}^{(\pi/2)}}{L}\left(1 - \frac{G_e^{(\pi/2)}}{G_e^{(\pi)}}\right)\Omega_1\right].z, \end{aligned} \tag{8}$$

which possesses the overall spatial dependence required by single-scan 2D NMR.

It is interesting to compare this final encoding expression with similar phase- and amplitude-modulation expressions derived for the cases of the discrete and the π/2–π/2 encodings; Eqs. (1) and (3), respectively [5,10]. As in these previous cases, Eq. (8) displays a z-independent term that, having a component proportional to $t_{1,\max}^{(\pi/2)}\Omega_1/2$, will impart a large first-order phase distortion on the peaks. To avoid dealing with this distortion we shall present, as was also done in previous publications, all experimental spectra in a magnitude representation. As for the linear z term in Eq. (8) this entails now an Ω_1-independent contribution, amounting to an offset along the indirect domain that was absent in the previous encoding modes. This offset arises from the unbalanced action of the encoding $G_e^{(\pi/2)}$ and $G_e^{(\pi)}$ gradients; its effects can easily be calculated a priori and compensated if needed via the setting of an appropriate offset during the chirped irradiation, or via the action of a suitable purging gradient prior to the actual data acquisition. Either route is without major complications; the latter was implemented in the experimental demonstrations detailed below. Also interesting to note is the value of the C spatio-temporal coefficient characterizing this new encoding mode: as in Eqs. (1) and (3) it is of the form $t_{1,\max}^{(\pi/2)}/L$, yet now scaled by a $[1 - G_e^{(\pi/2)}/G_e^{(\pi)}]$ factor. We discuss next how this new scaling contribution offers the possibility to perform a number of different single-scan 2D variants.

3. Results and discussion

3.1. Shift-optimized acquisitions: sensitivity-enhanced TOCSY and H,H-COSY

Among the experiments that are beyond the capabilities of amplitude-modulated sequences but within the reach of the scheme introduced in Fig. 1C is sensitivity-enhanced TOCSY [16,17], a homonuclear correlation experiment where an isotropic mixing sequence is employed to transfer both x and y components of magnetizations among I and J spins forming part of the same mutually coupled system. This dual $I_x \to J_x$, $I_y \to J_y$ transfer is to be contrasted against the single $I_\alpha \to J_\alpha$ component that will be transferred if an intermediate storage is performed, and which is known to lead to a sensitivity reduction in the resulting 2D correlation spectrum. To assess this potential difference two homonuclear single-scan 2D TOCSY ^{1}H NMR acquisitions were collected: one relying on the amplitude-modulated approach depicted in Fig. 1B, the other on the phase-modulated approach in Fig. 1C with $G_e^{(\pi)}$ set to 10 $G_e^{(\pi/2)}$. An n-butylchloride/$CDCl_3$ sample and the processing we have described elsewhere for ultrafast NMR acquisitions [5] were employed in both cases; as in all remaining instances discussed in this work a Varian iNova 500 MHz NMR spectrometer was employed for the actual experiments. Fig. 2 compares the results obtained in these 2D TOCSY tests. Upon setting equivalent total evolution times and C factors the overall spectral appearance of the two 2D data sets is naturally similar, even if the quality of the echo shapes in the amplitude-modulated approach seems slightly higher. On the other hand, an average signal enhancement of ≈2 characterized the phase-modulated data over its amplitude-modulated counterpart. This enhancement is what could be expected in terms of the magnetization storage implied by Eq. (3), which will scale encoded and

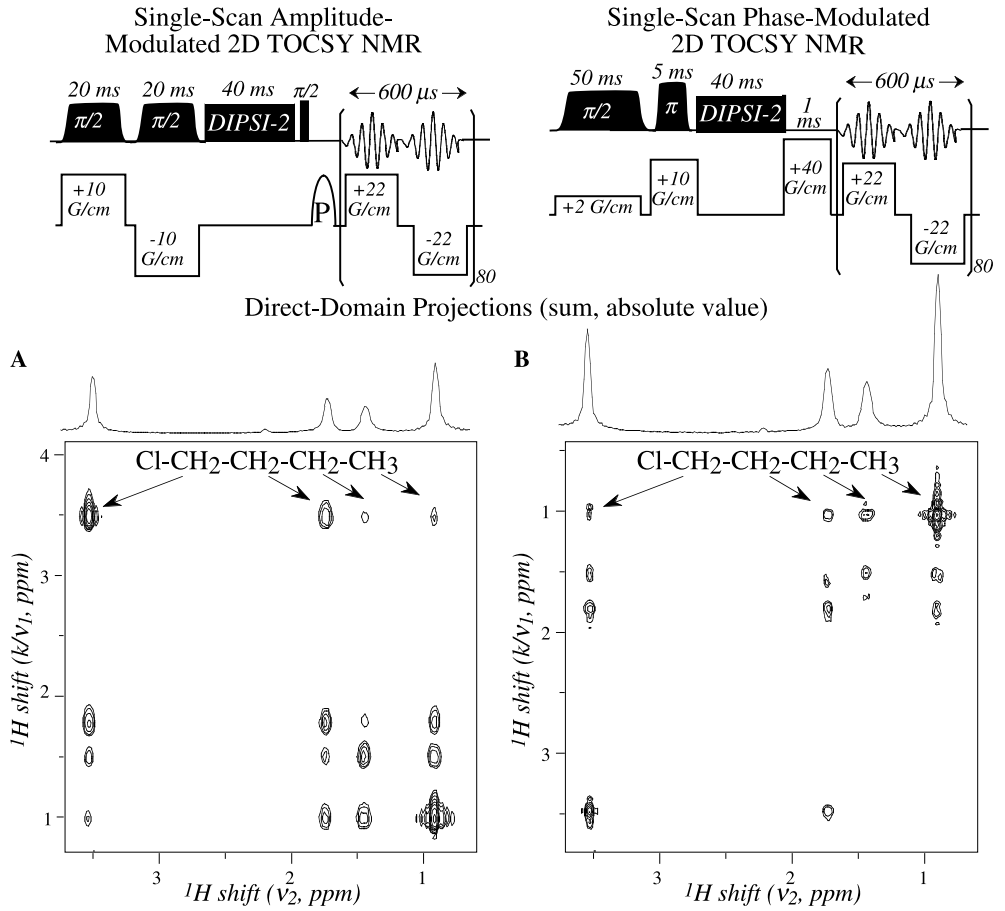

Fig. 2. Comparison between single-scan 2D TOCSY NMR spectra acquired on an *n*-butylchloride/$CDCl_3$ sample, utilizing the amplitude-modulated (A) and the phase-modulated (B) pulse sequences indicated on top. Also shown for the sake of a sensitivity comparison are the projections obtained in each instance upon adding up all points along the indirect dimension (shown in absolute intensity mode). Most of the experimental parameters are indicated in the figure and derive from the principles explained in [10] and in Section 2, leading to effective $t_1^{\max}$ encoding times of 40 and 45 ms in (A) and (B), respectively. Additional relevant parameters were gradient switching times of 10 μs, an $L = 1.8$ cm sample length, and a 40 ms long DIPSI-2-type sequence applied in the absence of gradients and over a 15 kHz bandwidth for the mixing. Also important to note are the $\gamma_e B_1$ settings used for the π/2 and π RF pulses: 200 and 1200 Hz, respectively. The value used for the π/2 chirp derives from the analysis given in [20]: $\gamma_e B_1^{(\pi/2)} = \sqrt{0.16|R^{(\pi/2)}|}$ with $R^{\pi/2} = \gamma_e G_e^{(\pi/2)} L / t_{1,\max}^{(\pi/2)}$; the π nutation was set up to fulfill with adiabatic passage requirements. WURST-50 RF shapes were used for all chirped pulses, with amplitudes and phases programmed in real time using Varian's Pbox subroutine libraries at a 1.5 μs digitization dwell. Processing involved a separation of the sampled data points into $+G_a$ and $-G_a$ contributions; then subjecting of one of these sets to zero-filling (140×128 (k, t_2)-points), FT against t_2, and magnitude calculation. Notice that as a result of the phase inversion involved when utilizing the π/2–π pulse scheme, its ν_1 indirect spectral domain appears reversed with respect to that arising from its π/2–π/2 counterpart upon being read out with the same G_a decoding gradient.

anti-encoded windings by a 1/2 factor. All remaining aspects of the phase-modulated experiment were also as expected including a reversal of the indirect-domain's frequency axis, the appearance of an additional offset for the k/ν_1 echoes, the magnitude of the C scaling values, the absence of "ghosting" effects, and the capacity of the spatial winding to be decoded by a $+G_a$ gradient but not by a $-G_a$ one.

A second application worth discussing concerns the implementation of single-scan homonuclear 2D COSY acquisitions. Such experiments were shown possible when using a discrete spatial encoding [4,5]; as illustrated in Fig. 3, they are also compatible with the π/2–π scheme introduced in this work. Once again, the $t_{1,\max}^{(\pi/2)} G_e^{(\pi/2)} = 2t_{1,\max}^{(\pi)} G_e^{(\pi)}$ and $G_e^{(\pi)} \approx 10 G_e^{(\pi/2)}$ conditions were chosen for setting up the indirect-domain encoding; this time followed by a hard π/2 pulse imparting the $2I_z J_\alpha \rightarrow 2I_\alpha J_z$ inter-site mixing, and then by the standard ultrafast 2D NMR acquisition. When subjecting an *n*-butylchloride/$CDCl_3$ sample to this kind of analysis, the nearest-neighbor cross-peak patterns expected for this simple compound were clearly discerned (Fig. 3B). Also in this instance the remaining aspects of the experiment were as expected. A sole minor discrepancy concerned the $G_e^{(\pi)}$ value, which sometimes yielded the sharpest echo peaks when slightly weaker than its ideal expectation. This in turn is not entirely surprising, giving the various approximations involved in the derivation of Eq. (7).

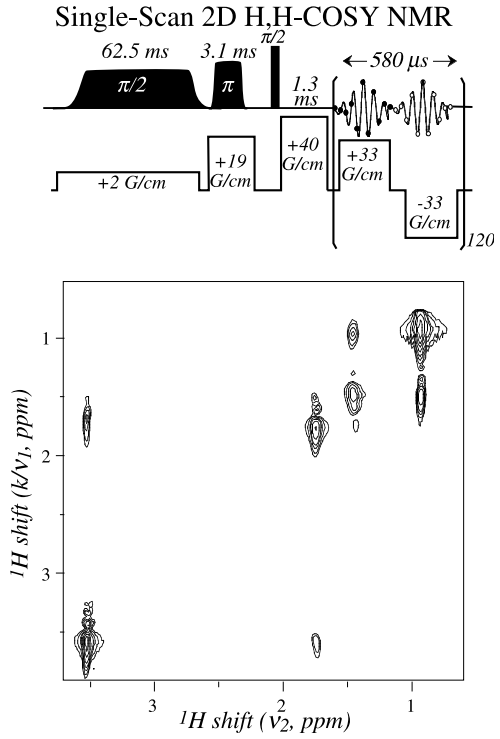

Fig. 3. Single-scan 2D H,H-COSY NMR spectrum acquired on an *n*-butylchloride/$CDCl_3$ sample, utilizing the π/2–π sequence illustrated on top. The final π/2 pulse was 7.4 μs long; all remaining pulse sequencing considerations were as in Fig. 2B. The acquired data points were separated for their off-line processing, zero-filled to 140×256 (k,t_2)-points, FT against t_2, and plotted in magnitude mode. Notice that for the sake of optimizing echo lineshapes, the $G_e^{(\pi)}$ value used in this experiment was set ca. 5% smaller than the ideal prediction of Eq. (7).

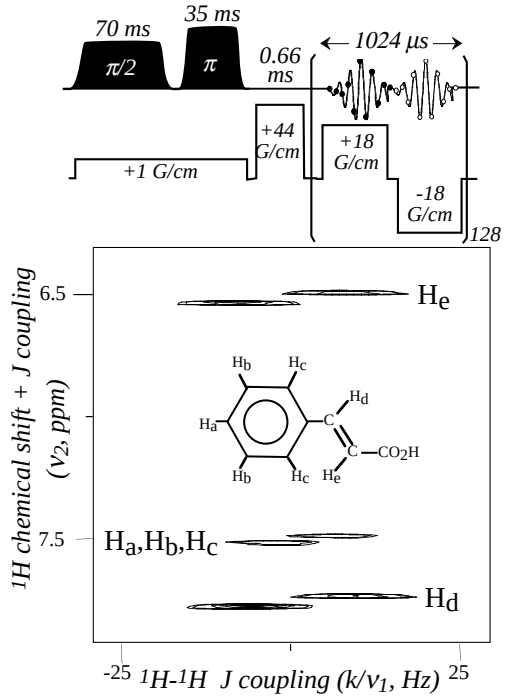

Fig. 4. (Top) Pulse sequence capable of affording a single-scan 2D *J*-resolved NMR spectrum, utilizing a continuous π/2–π phase encoding of the homonuclear coupling along the indirect domain. (Bottom) Results illustrating the pulse sequence's performance on a cinnamic acid/DMSO-d_6 solution, acquired with the various indicated parameters. Other setup and processing parameters of the single-scan data were akin to those in Figs. 2B and 3; notice the clearly discernible *J*-patterns for the various chemically inequivalent sites in the molecule.

3.2. Coupling-optimized acquisitions: 2D J-resolved spectroscopy

An interesting variant of the π/2–π encoding scheme arises when the condition in Eq. (7) is fulfilled, under conditions which make the spatio-temporal *C* factor in Eq. (8) simultaneously null. That is when encoding gradients are set $G_e^{(\pi/2)} = G_e^{(\pi)}$, while chirped pulse widths are set $t_{1,\max}^{(\pi/2)} = 2t_{1,\max}^{(\pi)}$. One then ends up with a situation where, apart from an a priori site-independent offset, the net effects of both the external gradients as well as of the internal chemical shifts are refocused. This is not to mean, however, that all interactions have necessarily been erased. In particular, the homonuclear *J* evolution, which being a scalar will remain unaffected by the application of a refocusing π pulse, will end up accumulating from the instant when a given spin packet becomes excited onwards. Unlike what happens with gradients and chemical shifts its spatial encoding effects will thus resist refocusing, and become imparted with an efficiency depending on $C = t_{1,\max}^{(\pi/2)}/L$. This indirect-domain pure-*J* winding pattern can then be read out in the usual ultrafast fashion via the action of oscillating $\pm G_a$ gradients, and correlated with the chemical-shift/*J*-coupling interactions characterizing the spins' free evolution along a direct t_2 domain. As a result of this correlation the characteristic pattern of a 2D *J*-resolved spectrum [3,11] will arise; Fig. 4 illustrates an example of this hitherto unexplored aspect of ultrafast 2D NMR's potential. Targeted in this experiment was a solution of cinnamic acid in DMSO-d_6, whose single-scan spectrum clearly reveals the differing *J* fine structures arising from the strongly coupled olefinic sites vis-à-vis the more weakly coupled aromatic ones. It is interesting note that a suitable shearing of this kind of 2D data sets along an appropriate angle could yield a homonuclear-decoupled, pure chemical shift spectrum within a single scan—a long sought yet hitherto elusive goal in ^{1}H solution-state NMR spectroscopy [22].

4. Outlook

As a number of approaches have already been introduced to achieve the spatial encoding required by ultrafast 2D NMR [4,10,23] we briefly dwell on assessing the potential benefits stemming from the new approach hereby introduced, as well as on its drawbacks and

remaining challenges to be overcome. Worth mentioning first is the fact that the proposed encoding scheme fulfills the main objective that it was set out to achieve: to provide a technologically simple phase-encoded spatial approach which, by avoiding repetitive oscillations of the auxiliary encoding gradient, is compatible with NMR systems prone to parasitic eddy currents—including cryogenically cooled probeheads as well as a majority of animal and human imaging systems. Indeed from a standpoint of gradient demands, it is unlikely that spatial encoding sequences much simpler than the one exemplified in Fig. 4 could be devised. Moreover, as was also the case for the amplitude-modulated scheme previously proposed, the present phase-modulated scheme manages to avoid certain artifacts that may characterize discrete spatial encoding procedures, including "ghost" fold-overs and "enveloping" effects. Yet unlike the amplitude-modulated scheme, the $\pi/2$–π approach hereby discussed is easily amenable to incorporation into 2D (and in general nD) NMR pulse sequences operating on the basis of single- or multiple-quantum coherence transfers.

Having listed these most evident advantages of the new approach, it is also worth dwelling in what—at least at this point—we perceive as some of its pitfalls. A relatively minor inconvenience relates to the distorted lineshapes that the new phase-encoded approach will provide, which will mix absorptive and dispersive components. Unlike what happened with the amplitude-modulated counterparts getting rid of these artifacts via an encoded/anti-encoded single-scan acquisition scheme will no longer be possible [8]; nonetheless, we shall describe elsewhere a minor modification that endows both amplitude- and phase-modulated schemes with the capability of eliminating dispersive and out-of-phase artifacts—always while remaining within a single scan. A more fundamental limitation worth assessing concerns the performance of the new encoding scheme in terms of that all-important aspect of single-scan 2D NMR: spectral sensitivity. In particular, if considering the potential effects of extensive molecular diffusion or body motions, few ultrafast 2D NMR schemes can be expected to receive a more substantial sensitivity hit during their encoding stages than the one in Fig. 4—which relies on the application of a weak but constant field gradient. In this respect it is difficult to conceive schemes better sheltered against displacement artifacts than those relying on discrete excitation pulses applied in synchrony with rapid $\pm G_e$ reversals of the gradients. Hence lies somewhat of a paradox in terms of the potential biomedical usage of ultrafast 2D NMR: encoding schemes which end up being easiest to implement on currently available MRI hardware, are also the most likely to be prone to artifacts upon the onset of motions—which are of course a common feature in in vivo spectroscopy. We are currently looking for compromises capable of solving this dichotomy, and yield implementations that are both instrumentally simple and insensitive to motions.

Acknowledgments

We are grateful to Dr. W. Kockenberger (University of Nottingham, UK) for sharing insight into his developments in this area. This work was supported by the Israel Science Foundation (Grant 296/01), by the U.S. National Institute of Health (GM72565), and by the German-Israel Fund for Research (GIF 56/2003).

References

[1] J. Jeener, Lecture presented at Ampere International Summer School II, Basko Polje, Yugoslavia, September 1971
[2] W.P. Aue, E. Bartholdi, R.R. Ernst, Two dimensional spectroscopy. Application to nuclear magnetic resonance, J. Chem. Phys. 64 (1976) 2229–2246.
[3] R.R. Ernst, G. Bodenhausen, A. Wokaun, Principles of Nuclear Magnetic Resonance in One and Two Dimensions, Clarendon Press, Oxford, 1987.
[4] L. Frydman, T. Scherf, A. Lupulescu, The acquisition of multidimensional NMR spectra within a single scan, Proc. Natl. Acad. Sci. USA 99 (2002) 15858–15862.
[5] L. Frydman, A. Lupulescu, T. Scherf, Principles and features of single-scan two-dimensional NMR spectroscopy, J. Am. Chem. Soc. 125 (2003) 9204–9217.
[6] Y. Shrot, L. Frydman, Single-scan NMR spectroscopy at arbitrary dimensions, J. Am. Chem. Soc. 125 (2003) 11385–11396.
[7] Y. Shrot, L. Frydman, Spatially resolved multidimensional NMR spectroscopy within a single scan, J. Magn. Reson. 167 (2004) 42–48.
[8] B. Shapira, A. Lupulescu, Y. Shrot, L. Frydman, Line shape considerations in ultrafast 2D NMR, J. Magn. Reson. 166 (2004) 152–164.
[9] M. Mishkovsky, L. Frydman, Interlaced fourier transformation of ultrafast 2D NMR data, J. Magn. Reson. 173 (2005) 344–350.
[10] Y. Shrot, B. Shapira, L. Frydman, Ultrafast 2D NMR spectroscopy using a continuous spatial encoding of the spin interactions, J. Magn. Reson. 171 (2004) 162–169.
[11] W.P. Aue, J. Karhan, R.R. Ernst, Homonuclear broadband decoupling and 2D J-resolved NMR spectroscopy, J. Chem. Phys. 64 (1976) 4226–4227.
[12] M.A. Thomas, L.N. Ryner, M.P. Mehta, P.A. Turski, J.A. Sorenson, Localized 2D J-resolved ^{1}H MR spectroscopy of human brain, J. Magn. Reson. Imaging 6 (1996) 453–459.
[13] M.G. Swanson, D.B. Vigneron, T.-K.C. Tran, R.E. Hurd, J. Kurhanewicz, Single voxel oversampled J-resolved spectroscopy of in vivo human prostate tissue, Magn. Reson. Med. 45 (2001) 973–980.
[14] M.A. Thomas, K. Yue, N. Binesh, P. Davanzo, A. Kumar, B. Siegel, M. Frye, J. Curran, R. Lufkin, P. Martin, B. Guze, Localized two-dimensional shift correlated MR spectroscopy of human brain, Magn. Reson. Med. 46 (2001) 58–67.
[15] A. Ziegler, B. Gillet, J. Beoeil, J. Macher, M. Decorps, J. Nedelec, Localized 2D correlation spectroscopy in human brain at 3T, MAGMA 14 (2002) 45–49.

[16] L. Braunschweiler, R.R. Ernst, Coherence transfer by isotropic mixing: application to proton correlation spectroscopy, J. Magn. Reson. 53 (1983) 521–528.
[17] J. Cavanagh, M. Rance, Sensitivity improvements in isotropic mixing experiments, J. Magn. Reson. 88 (1990) 72–85.
[18] L.E. Kay, P. Keifer, T. Saarinen, Pure absorption gradient enhanced heteronuclear single quantum correlation spectroscopy with improved sensitivity, J. Am. Chem. Soc. 114 (1992) 10663–10665.
[19] G. Kontaxis, J. Stonehouse, E.D. Laue, J. Keeler, The sensitivity of experiments which use gradient pulses for coherence pathway selection, J. Magn. Reson. Ser. A 111 (1994) 70–76.
[20] Y. Shrot, L. Frydman, Spatially encoded NMR and the acquisition of 2D magnetic resonance images within a single scan, J. Magn. Reson. 172 (2005) 179–190.
[21] M. Garwood, L. DelaBarre, The return of the frequency sweep: designing adiabatic pulses for contemporary NMR, J. Magn. Reson. 153 (2001) 155–177.
[22] See, for instance R. Freeman, Spin Choreography: Basic Steps in High Resolution NMR, Oxford University Press, Oxford, 1998, Paragraph 8.5 and references therein.
[23] P. Pelupessy, Adiabatic single-scan 2D NMR spectroscopy, J. Am. Chem. Soc. 125 (2003) 12345–12350.